Original Article

Gut microbiota and metabolites associated with immunotherapy efficacy in extensive-stage small cell lung cancer: a pilot study

Liyang Sun[1#^], Xueting Wang[1#], Huimin Zhou[1#], Rui Li[2], Ming Meng[3], Giandomenico Roviello[4], Byeongsang Oh[5], Lingxin Feng[1], Zhuang Yu[1], Jing Wang[1]

[1]Department of Oncology, the Affiliated Hospital of Qingdao University, Qingdao University, Qingdao, China; [2]Health Management Center, the Affiliated Hospital of Qingdao University, Qingdao University, Qingdao, China; [3]School of Pharmacy, Qingdao University Medical College, Qingdao University, Qingdao, China; [4]Department of Health Sciences, University of Florence, Florence, Italy; [5]Northern Sydney Cancer Centre, Royal North Shore Hospital, University of Sydney Medical School, Sydney, NSW, Australia

Contributions: (I) Conception and design: J Wang; (II) Administrative support: Z Yu; (III) Provision of study materials or patients: J Wang, Z Yu, L Feng; (IV) Collection and assembly of data: L Sun, H Zhou; (V) Data analysis and interpretation: L Sun, H Zhou, X Wang, M Meng; (VI) Manuscript writing: All authors; (VII) Final approval of manuscript: All authors.

[#]These authors contributed equally to this work.

Correspondence to: Jing Wang, PhD; Zhuang Yu, PhD. Department of Oncology, the Affiliated Hospital of Qingdao University, Qingdao University, No. 59 Haier Road, Laoshan District, Qingdao 266000, China. Email: wangstella2021@qdu.edu.cn; yuzhuang2002@163.com.

Background: The gut microbiota and its associated metabolites play a critical role in shaping the systemic immune response and influencing the efficacy of immunotherapy. In this study, patients with extensive-stage small cell lung cancer (ES-SCLC) were included to explore the correlation between gut microbiota and metabolites and immunotherapy efficacy in patients with ES-SCLC.

Methods: Pre- and post-treatment, we collected stool samples from 49 ES-SCLC patients treated with an anti-programmed death-ligand 1 (PD-L1) antibody. We then applied 16S ribosomal RNA (rRNA) sequencing and liquid chromatography-mass spectrometry (LC-MS) non-targeted metabolomics technology. Subsequently, the gut microbiota and metabolites were identified and classified.

Results: The results showed no statistical difference in gut microbiota alpha and beta diversity between the responder (R) and non-responder (NR) patients at baseline. However, the alpha diversity of the R patients was significantly higher than that of the NR patients after treatment. There were also differences in the microbiome composition at the baseline and post-treatment. Notably, after treatment, *Faecalibacterium*, *Clostridium_sensu_stricto_1*, and *[Ruminococcus]_torques* were enriched in the R group, while *Dubosiella*, *coriobacteriaceae_UCG-002* was enriched in the NR group. The non-targeted metabolomics results also indicated that short-chain fatty acids (SCFAs) were up-regulated in the R group after treatment. More, differential metabolites were enriched in the Kyoto Encyclopedia of Genes and Genomes (KEGG) pathways, including the PD-L1 expression and programmed death 1 (PD-1) checkpoint pathway in cancer.

Conclusions: These findings are anticipated to provide novel markers for predicting the efficacy of immune checkpoint inhibitors (ICIs) in patients with ES-SCLC, and offer new directions for further research on molecular mechanisms.

Keywords: Small cell lung cancer (SCLC); gut microbiota; metabolomics; immunotherapy; chemotherapy

Submitted Jul 26, 2024. Accepted for publication Sep 13, 2024. Published online Oct 14, 2024.
doi: 10.21037/jtd-24-1201
View this article at: https://dx.doi.org/10.21037/jtd-24-1201

^ ORCID: 0009-0007-8143-0836.

Introduction

Lung cancer (LC) is one of the most prevalent and fatal malignancies worldwide, and its incidence and mortality rates continue to increase (1). In 2023, there were more than 238,000 new LC cases and 127,000 LC-related deaths in the United States (1). Small cell LC (SCLC) accounts for approximately 15% of all LC cases, and is characterized by an unconventionally high proliferative rate, a strong tendency for early widespread metastasis, and acquired chemoresistance (2). Approximately 70% of SCLC cases present with extensive-stage SCLC (ES-SCLC) at the time of diagnosis (3). Over the past three decades, etoposide combined with platinum chemotherapy has been recommended as the first-line treatment for ES-SCLC patients. However, the clinical benefit of ES-SCLC treatments is still not as favorable as that achieved by non-SCLC (NSCLC) treatments, and ES-SCLC patients have a worse prognosis than those NSCLC patients. Immune checkpoint inhibitors (ICIs), especially those that block the programmed death 1 (PD-1)/programmed death-ligand 1 (PD-L1) axis, have recently provided a new therapeutic approach for SCLC. Indeed, the National Comprehensive Cancer Network (NCCN), Chinese Society of Clinical Oncology (CSCO), and American Society of Clinical Oncology (ASCO) guidelines all recommend an ICI anti-PD-L1 antibody combined with chemotherapy as the first-line treatment for ES-SCLC (4-6). Thus, ICIs represent an important advancement in the treatment of SCLC patients. Despite the great clinical achievements of ICIs, predicting who will respond to ICIs has proven to be difficult, and new predictive immunotherapy biomarkers need to be discovered (7). Further, resistance to ICIs in SCLC is frequent either because of a lack of response or disease progression after an initial response (3). Therefore, to maximize the benefits for SCLC patients, biomarkers need to be explored to guide the selection of immunotherapy patients. However, to date, these aspects have remained largely unexplored.

Accumulating evidence has shown that the occurrence and development of LC are related to the human gut microbiome, and the interaction between these microbiomes influences the functioning of multiple pathways, including the inflammatory and immune pathways (8-10). The connection between the human gut microbiome and clinical responses to anti-PD-1/PD-L1 treatment has become apparent in recent years (11,12), and the gut microbiota has been shown to play a critical role in ICI treatment for advanced melanoma (13), NSCLC (14), and advanced renal cell cancer (15). Furthermore, a study has also reported a strong relationship between microbiota-derived metabolites and immunotherapy (16). Notably, research has shown that microbiota-derived metabolites modulate multiple human physiologies and spread from their original location in the gut to mediate local and systemic anti-tumor immune responses to promote ICI efficacy (16). These metabolites affect the efficacy of immunotherapy through several mechanisms, including by providing metabolic energy, promoting biosynthesis, and altering signaling proteins (17,18). However, understandings of the interactions between the gut microbiota and metabolites and how they affect the treatment of SCLC with ICIs are poor.

In this study, we analyzed the differences in the gut microbiome and metabolites of patients with ES-SCLC and how they are related to ICI treatment. Specifically, we used 16S ribosomal RNA (rRNA) gene sequencing and non-targeted metabolomics techniques to gain a better understanding of the gut microbiota and metabolites during ICI treatment. We collected fecal samples from the baseline to the end of ICI treatment and examined changes in the gut microbiota and metabolites to gain a comprehensive understanding of how they were correlated with efficacy. This is the first report to explore potential biomarkers of benefit for ES-SCLC patients receiving immunotherapy by studying the correlation between the gut microbiota and metabolites and treatment efficacy in patients treated with anti-PD-L1 agents. We present this article in accordance with the MDAR reporting checklist (available at https://jtd.

Highlight box

Key findings

- Gut microbiota and metabolites influence the efficacy of immunotherapy in small cell lung cancer (SCLC).

What is known, and what is new?

- Previous studies have shown that gut microbiota and metabolites influence the efficacy of immunotherapy for non-SCLC, renal cell carcinoma, and other tumors.
- Many genera and metabolites also influence the efficacy of immunotherapy in SCLC.

What is the implication, and what should change now?

- Our findings may provide additional research directions for SCLC immunotherapy.
- Whether or not to apply immune checkpoint inhibitors for extensive-stage SCLC patients should be based on the gut microbiota.

amegroups.com/article/view/10.21037/jtd-24-1201/rc).

Methods

Patient characteristics

A total of 60 patients with ES-SCLC who received immunotherapy combined with chemotherapy as the primary treatment at the Affiliated Hospital of Qingdao University from June 2020 to June 2023 were enrolled in this study. And the enrolled ES-SCLC patients received chemotherapy regimens of etoposide (100–120 mg/m^2, days 1–3) combined with carboplatin [area under the curve (AUC) 5–6, day 1] or cisplatin (60–75 mg/m^2, day 1), and immunosuppressants of durvalumab [1,500 mg, every 3 weeks (q3w)] or atezolizumab (1,200 mg, q3w). To be eligible for inclusion in this study, the patients had to meet the following inclusion criteria: (I) have been diagnosed with ES-SCLC as per the Manual of the International Association for the Study of Lung Cancer, Staging Manual for Thoracic Oncology, 8th edition; (II) be aged 18 years of age or older; and (III) have an Eastern Cooperative Oncology Performance Status score of ≤1. Patients were excluded from the study if they met any of the following exclusion criteria: (I) had taken immunostimulants, antibiotics, probiotics, prebiotics, or corticosteroids within the past 3 months; and/or (II) had experienced any other gastrointestinal diseases and active immunological disease within the past 3 months. The study was approved by the Ethics Committee of the Affiliated Hospital of Qingdao University (ethics number: QYFY WZLL 27469), and it was conducted in accordance with the Declaration of Helsinki (as revised in 2013). All the patients were informed of the study and provided informed consent.

After the final exclusion of patients who were lost to follow-up, 49 patients remained, of whom 37 were male and 12 were female. All the patients enrolled in the study received chemotherapy combined with anti-PD-L1 immunotherapy with or without palliative radiotherapy for bone and brain metastases. Responses to treatment were assessed after every two cycles of treatment, and were confirmed by a subsequent assessment no less than 4 weeks from the date first documented. The Response Evaluation Criteria in Solid Tumors version 1.1 (RECIST 1.1) was strictly followed. Responses were categorized as a complete response (CR), partial response (PR), stable disease (SD), and progressive disease (PD). Given the high degree of malignancy in ES-SCLC, rapid disease progression, and short median survival time of such patients (7), the responder (R) and non-responder (NR) patients were defined by whether the duration of the response was ≥6 months; patients in the R group comprised those with a CR + PR + SD duration of ≥6 months, while patients in the NR group comprised those who experienced disease progression within 6 months of the start of ICI treatment (14).

Fecal sample collection and processing

Fecal samples were initially collected once before the treatment (t0) and were then continuously collected after every two cycles of treatment but before immunotherapy infusion. The last treatment time of patients in group R was t1, and the last evaluation time of patients in group NR was t1. The collected fresh samples were stored in sterile containers and kept at −80 ℃. And 16S rRNA sequencing was performed in all patients after 6 months of follow-up.

16S rRNA sequencing and topological analysis of the gut microbiome

The E.Z.N.A.® Soil DNA Kit (Omega Bio-tek, Norcross, GA, USA) kit was used to extract DNA, and 1% agarose gel electrophoresis was then used to detect the extracted genomic DNA in accordance with the manufacturer's instructions. The V3–V4 region of the 16s rRNA coding gene was amplified from the extracted DNA using barcoded double-indexed primers. Three replicates were set up for each sample, and the polymerase chain reaction products were identified by gel electrophoresis, purified by the AxyPrep DNA Gel Extraction Kit (Axygen, Silicon Valley, CA, USA), and quantified using the Quantus™ Fluorometer (Promega, Madison, WI, USA). DNA was then constructed and sequenced using the TruSeqTM DNA Sample Prep Kit (Illumina, San Diego, CA, USA), and operational taxonomic units (OTUs) with a sequence similarity of ≥97% were defined as classification units. The characteristic sequences of each representative sequence were annotated using the SILVA database (http://www.arb-silva.de), and the representative sequences of each OTU were classified and annotated with a 0.7 confidence threshold, and the OTU sequences were then clustered and analyzed with Uprase (http://www.drive5.com/uparse/). The OTU sequences were optimized and subjected to a taxonomic analysis and beta diversity analysis using Qiime (http://qiime.org/install/index.html). The alpha diversity analysis, including the Chao1 index and Shannon index analyses, was performed on

the Mothur platform (http://mothur.org/wiki/Download_mothur), while the beta diversity analysis was performed by weighted UniFrac principal coordinate analysis (PCoA) using the UniFrac distance matrix of the Qiime platform. PICRUST2 (https://github.com/picrust/picrust2/) was used to perform the Kyoto Encyclopedia of Genes and Genomes (KEGG) functional annotation of the intestinal flora.

Metabolomics analysis

The 100-µL sample was transferred into an Eppendorf (EP) tube, and 300 µL of extraction solution (methanol, isotopically labeled internal standard mixture) was added. The mixture was swirled for 30 seconds, then subjected to ultrasound for 10 minutes in an ice water bath, and left to stand at −40 ℃ for 1 hour. Afterward, the sample was centrifuged at 12,000 rpm [centrifugal force: 13,800 ×g, radius: 8.6 cm] at 4 ℃ for 15 minutes. The supernatant was then transferred into a sample bottle for machine testing. All the samples were combined with an equal amount of supernatant to create quality control (QC) samples for machine testing.

The samples were analyzed using an UltiMate 3000 UHPLC Systems ultra-high performance liquid chromatography (UHPLC; Thermo Fisher Scientific, Waltham, MA, USA) with a Waters ACQUITY UPLC HSS T3 (2.1 mm × 100 mm, 1.8 µm) liquid chromatography column (Thermo Fisher Scientific). The chromatographic separation used an aqueous phase containing 5 mmol/L of ammonium acetate and 5 mmol/L of acetic acid (phase A), and acetonitrile (phase B). The sample plate temperature was maintained at 4 ℃, and 2 µL sample was used for injection. The Orbitrap Exploris 120 mass spectrometer (MS; Thermo Fisher Scientific) was used for the primary and secondary MS data acquisition under the control software Xcalibur (version 4.4; Thermo Fisher Scientific). The specific parameters included a sheath gas flow rate of 50 Arb, an Aux gas flow rate of 15 Arb, a capillary temperature of 320 ℃, full MS resolution of 60,000, MS/MS resolution of 15,000, collision energy in the normalized collision energy (NCE) mode of 10/30/60, and a spray voltage of 3.8 kV (positive) or −3.4 kV (negative).

Statistical analysis

The statistical analysis was performed using GraphPad Prism software v.9.5, Qiime. The sample baseline data were compared using the Wilcoxon test and Fisher exact test. An Adonis analysis, Wilcoxon rank-sum test, and Kruskal-Wallis test were used to compare differences between microbiomes. The metabolomics data were processed and analyzed using Progenesis QI v2.3 software (https://www.waters.com/nextgen/cn/zh/products/informatics-and-software/mass-spectrometry-software/progenesis-qi-software.html). The metabolites were compared between groups using the Wilcox test and a fold-change analysis. The Pearson correlation coefficient was used to measure the degree of linear correlation between two metabolites. Spearman's rank correlation test was used to assess the correlation between microorganisms and metabolites. A P value <0.05 indicated a statistically significant difference.

Results

Baseline characteristics and grouping scheme of ES-SCLC patients

Our study included 60 ES-SCLC patients hospitalized between June 2020 and June 2023. All the patients received chemotherapy with anti-PD-L1 immunotherapy, and 16 also received radiotherapy. Unfortunately, 11 patients were lost during follow-up. Of the remaining 49 patients, the R group (n=25) and NR group (n=24) were formed based on the clinical assessment (*Figure 1*). The majority of patients were male (75.5%), and there were no significant differences between the two groups in terms of age, gender, smoking status, body mass index, and radiotherapy history (P>0.05) (*Table 1*).

Characterization of the gut microbiome in patients with ES-SCLC in the R and NR groups

The patients were divided into the following two groups based on treatment efficacy: (I) the R group, which comprised patients who showed treatment efficacy (a CR, PR, or SD) for ≥6 months; and (II) the NR group, which comprised patients who showed disease progression within 6 months of treatment. A total of 3,844 OTUs were identified, including 948 core OTUs, and 308 OTUs unique to R_t0, R_t1, NR_t0, and NR_t1 (*Figure 2A*). At the phylum level, the major components of the gut microbiota were *Firmicutes*, *Bacteroidota*, *Proteobacteria*, and *Actinobacteriota* (*Figure 2B*). At the family level, *Lachnospiraceae* was the most common bacteria in all groups (*Figure 2C*). The most common genus in the R and NR groups before treatment was *Escherichia-Shigella*, while after

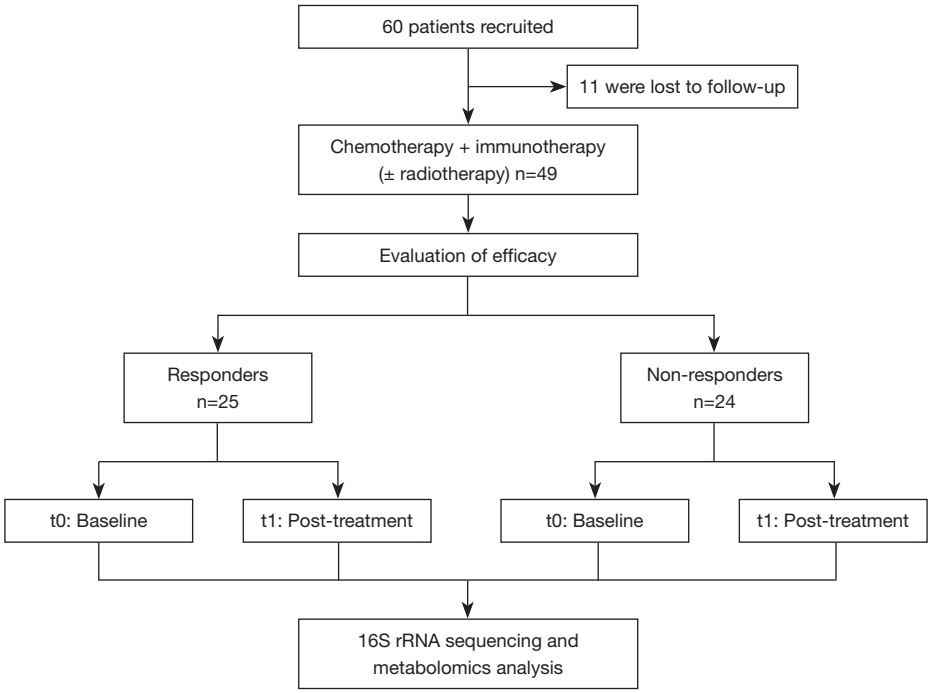

Figure 1 Study flowchart. rRNA, ribosomal RNA.

Table 1 Baseline characteristics of patients

Characteristics	R group (n=25)	NR group (n=24)	P value
Age (years)			0.32
>65	10	13	
≤65	15	11	
Gender			0.56
Male	18	19	
Female	7	5	
History of smoking			0.48
Yes	11	13	
No	14	11	
History of radiotherapy			0.61
Yes	9	7	
No	16	17	
Metastasis			0.51
Brain	3	7	
Bone	6	3	
Adrenal gland	2	4	
Liver	6	5	
Others	8	9	
Body mass index (kg/m^2)	23.81±3.67	23.77±3.00	0.97

Data are presented as n or mean ± standard deviation. R, responder; NR, non-responder.

treatment, the most common was *Blautia* in the R group, and *Escherichia-Shigella* in the NR group (*Figure 2D*).

Given that the abundance of *Firmicutes* and *Bacteroides* has been discovered to be related to the response to anti-PD-1 therapy in melanoma and NSCLC patients (19), we further generated bar charts for each group according to the percentage of *Firmicutes* and *Bacteroides* using the samples of each group. We found that the abundance of *Firmicutes* and *Bacteroidota* in the R group tended to increase after immunotherapy, but the decrease of the *Firmicutes* to *Bacteroides* (F/B) ratio was more obvious (*Figure 2E,2F*); the F/B ratios of group R and NR at the t0 and t1 time points were 13.527 (3.451/53.460) and 8.148 (1.692/280.658), respectively (*Figure 2G*).

Diversity indicators of the gut microbiome in patients with ES-SCLC in the R and NR groups

Subsequently, we used alpha and beta diversity indices to evaluate the microbial diversity of each group. As *Figure 3A,3B* show, alpha diversity was higher in the R group than the NR group at the baseline, but the difference was not statistically significant (*Figure 3A*: Chao1, P>0.05; *Figure 3B*: Shannon, P>0.05). At the t1 time point, the abundance of the gut microbiota of the R group was

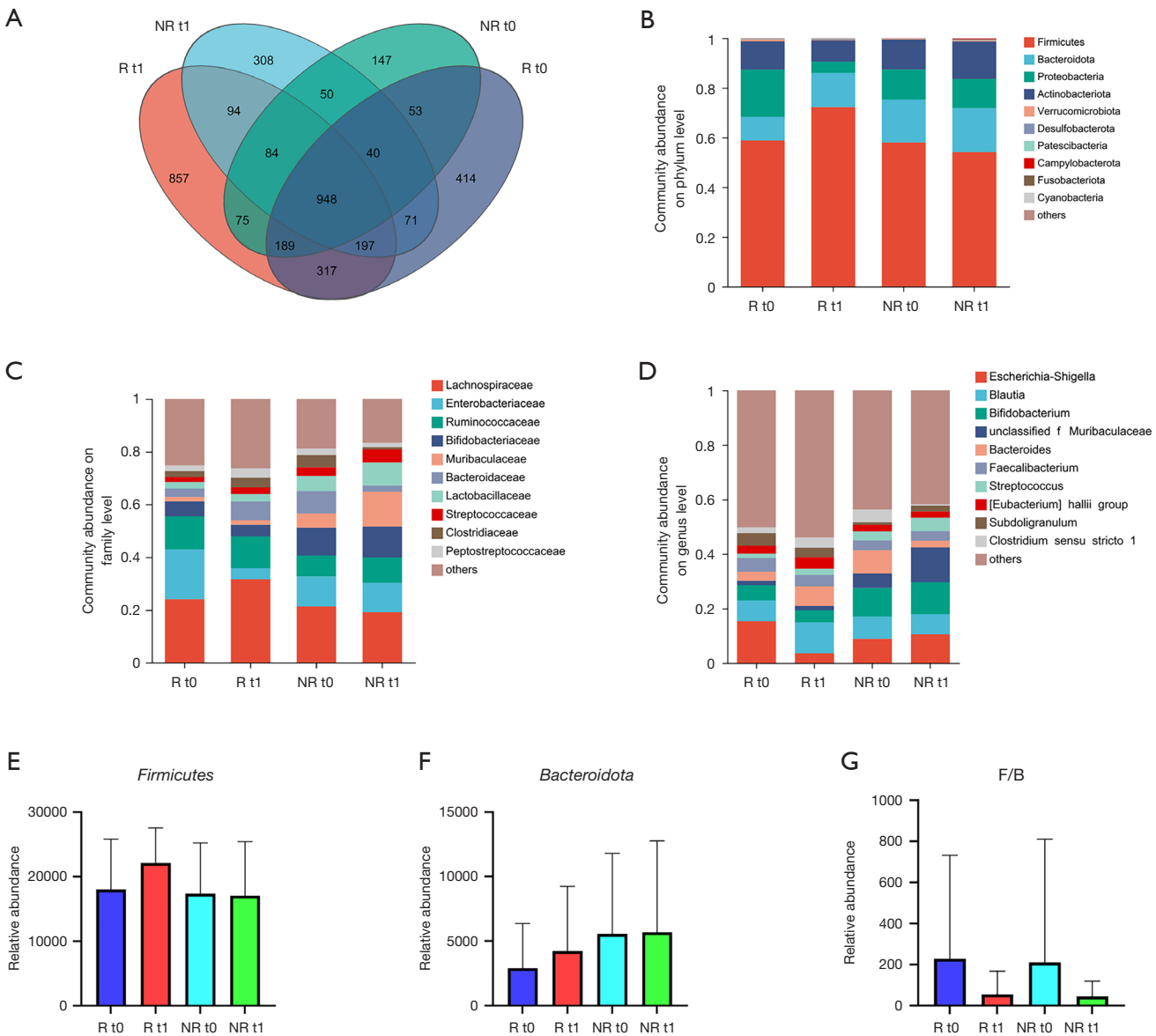

Figure 2 Comparison of gut microbiota composition between the R and NR groups. (A) Venn diagram showing each group of unique and common OTUs. (B) The top 10 representative species and their proportions in the four groups at the phylum level. (C) The top 10 representative species and their proportions in the four groups at the family level. (D) The top 10 representative species and their proportions in the four groups at the genus level. (E) Histogram of the representative *Firmicutes* differentially abundant in the R and NR groups. (F) Histogram of the representative *Bacteroidota* differentially abundant in the R and NR groups. (G) Histogram of the F/B difference trend. The statistical analysis was performed by the Mann-Whitney test. R, responder; NR, non-responder; t0, baseline; t1, post-treatment; F/B, *Firmicutes* to *Bacteroides*; OTU, operational taxonomic unit.

significantly higher than that of the NR group (*Figure 3C*: Chao1, P<0.05), while the diversity tended to increase, but the difference in the Shannon index was not significant between the two groups (*Figure 3D*: Shannon, P>0.05). These results indicate that the intra-individual bacterial abundance of the R patients differed to that of the NR patients.

We conducted a Bray-Curtis PCoA to compare the beta diversity between the two groups. No significant difference in beta diversity was found at the baseline (*Figure 3E*:

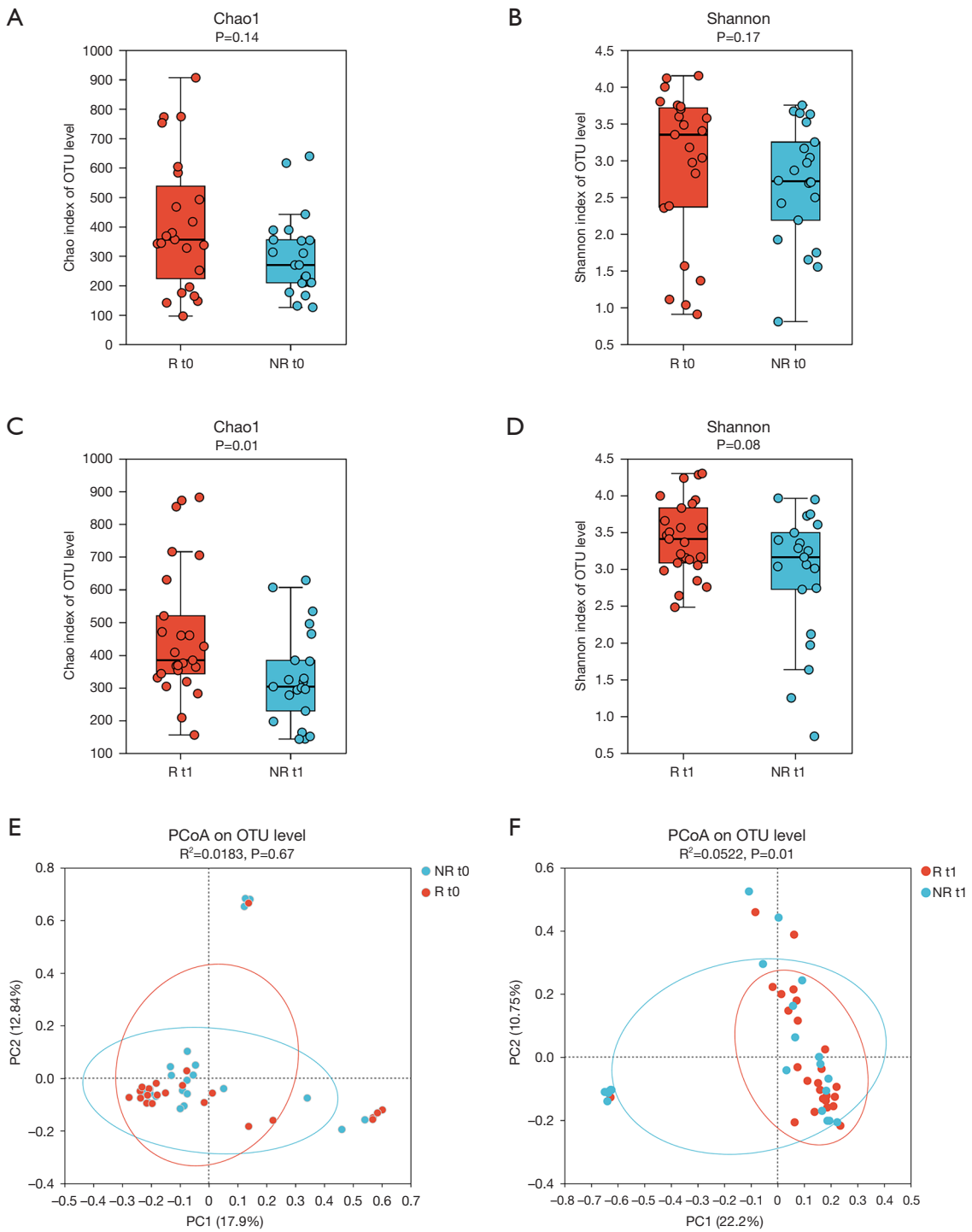

Figure 3 Comparison of gut microbiota diversity between the R and NR groups. (A,B) Chao1 index and Shannon index in the R and NR groups at the baseline. (C,D) Chao1 index and Shannon index in the R and NR groups at the t1 timepoint. (E,F) Beta diversity (as expressed by the PCoA) in the R and NR groups at the baseline (E) and at the t1 timepoint (F). The statistical analysis was performed by the Mann-Whitney test. OTU, operational taxonomic unit; R, responder; NR, non-responder; t0, baseline; t1, post-treatment; PC, principal component; PCoA, principal coordinate analysis.

P>0.05). However, after ICI treatment, a statistical difference in the PCoA was observed between the R and NR groups (*Figure 3F*: P<0.05). This indicates that the structural diversity of the gut microbiota may be related to immunotherapeutic efficacy. The insufficient sample size might explain the lack of statistical significance at the baseline.

Association between specific differential gut microbiota and ICIs response

Evolutionary plots were generated using linear discriminant analysis (LDA) effect sizes (LEfSe) to reveal differences in taxon abundance between the R and NR groups at the baseline and after treatment. At the baseline, 15 bacterial taxonomic branches differed significantly [$\log_{10}$(LDA score) >2] in the R and NR groups (*Figure 4A*,*4B*). At the baseline, in the R group. *f_Eggerthellaceae* was significantly elevated at the family level, and *Desulfovibrionaceae* and *Holdemanella* were also enriched at the genus level. In the NR group, there was no characteristic microbiome. As *Figure 4C*,*4D* show, after immunotherapy treatment *c_Clostridia* was an abundant taxon in the R group, and the prominent genera in the R_t1 group were mostly short-chain fatty acid (SCFA)-producing genera in *Firmicutes* or *Bacteroidota*, including *g_Clostridium_sensu_stricto_1*, *g_Romboutsia*, *g_Dorea*, *g_(Ruminococcus)_torques_*, *g_Subdoligranulum*, *g_Faecalibacterium*, *g_Prevotella_9*, *g_Phascolarctobacterium*, *g_Hungatella*, *g_Catenibacterium*, *g_Coprococcus*, *g_Oscillospira*, and *g_Butyricimonas*. *O_Lactobacillales* was the most abundant taxon in the NR_t1 group, and *g_Dubosiell*, *g_Alloprevotella*, and *g_Dubosiella* were the most prominent genus-level biomarkers. Overall, these findings suggest that the microbial abundance of the NR group was relatively lower than that of the R group at both the baseline and after treatment, which showed that the gut microbiota could serve as an important reference in distinguishing between patients who responded well to SCLC immunotherapy and those who responded relatively poorly.

In addition, we further refined significant differences in gut microbial expression abundance between the R and NR groups at the phylum and genus levels. At the baseline, the only significant difference between the two groups was *Desulfobacterota* at the phylum level (*Figure 4E*), which implies that patients with higher baseline *Desulfobacterota* abundance might have a better prognosis with immunotherapy. At the genus level, the following 12 genera had significantly higher bacterial abundance in the early R group than the NR group (P<0.05) (*Figure 4F*): *Unclassified_f_UCG-010*, *UCG-003*, *Biophila*, *Solobacterium*, *Unclassified_f_peptococcaceae*, *Unclassified_f_christensenellaceae*, *Parvimonas*, *Abiotrophia*, *Finegoldia*, *Propionibacterium*, and *UCG_007 Anaerococcus*. After treatment, the abundance of *Firmicutes* and *unclassified_d__Bacteria* was significantly higher in the R group than the NR group (P<0.05) (*Figure 4G*), and at the genus level, the following 13 genera of bacteria in the R group differed significantly (*Figure 4H*): *Faecalibacterium*, *Subdoligranulum*, *Clostridium_sensu_stricto_1*, *Dorea*, *Romboutsia*, *(Ruminococcus)_torques_*, *Coprococcus*, *Prevotella_9*, *Phascolarctobacterium*, *Monoglobus*, *unclassified_f_Ruminococcaceae*, *UCG-005*, and *Hungatella*. While in the NR group, *Dubosiella* and *Coriobacteriaceae_UCG-002* were relatively abundant at the genus level.

KEGG functional characteristics of the gut microbiome between groups

PICRUST2 was used to predict the biological functions of the microbiota using samples from the R and NR groups at the MetaCyc (http://www.genome.jp/kegg/) pathway level. As *Figure 5* shows, there was no significant difference in the relevant metabolic pathways at the baseline level between the two groups, but most of the pathways were enriched in the R group after the efficacy assessment, and the abundance of the flora involved in the functional pathways in the R group was increased compared to that in the pre-treatment period, and the functions were mainly focused on energy metabolism (e.g., NONOXIPENT-PWY, PWY-7111, ANAGLYCOLYSIS-PWY, PWY-5100, GLYCOGENSYNTH-PWY, and GLYCOCAT-PWY) and amino acid, nucleotide, and lipid biosynthesis (e.g., PWY-5101, PWY-5101, PWY0-1319, PWY-5667, ILEUSYN-PWY, VALSYN-PWY, and PWY-5104), and other pathways. While the NR group colonies were reduced in almost all of the above pathways compared to the baseline. These results suggest that the efficacy of immunotherapy may be associated with colonies that have functions in energy metabolism, the biosynthesis of amino acids, nucleotides, and so on.

Metabolomic signature of fecal samples in patients with ES-SCLC in the R and NR groups

To further explore changes in the gut-microbiome interaction with the treatment response, we performed a liquid chromatography-MS (LC-MS)-based non-targeted

metabolomic analysis of feces samples from the R and NR patients with ES-SCLC. A partial least squares discriminant analysis (PLS-DA) statistical analysis was used to screen for differential metabolites between the groups. The PLS-DA score plots showed significant differences between the R and NR groups at the baseline and after treatment. Next, differentially expressed metabolite ions were screened using Wilcox test P values and variable importance in the projection (VIP) values based on the following criteria: VIP ≥1.0, and P<0.05. A total of 259 different metabolites were identified in both groups at the baseline, and at t1, a total of 234 differential metabolites, including lipids and others, were found in both groups, most of which were down-regulated. A comparison with the Human Metabolome

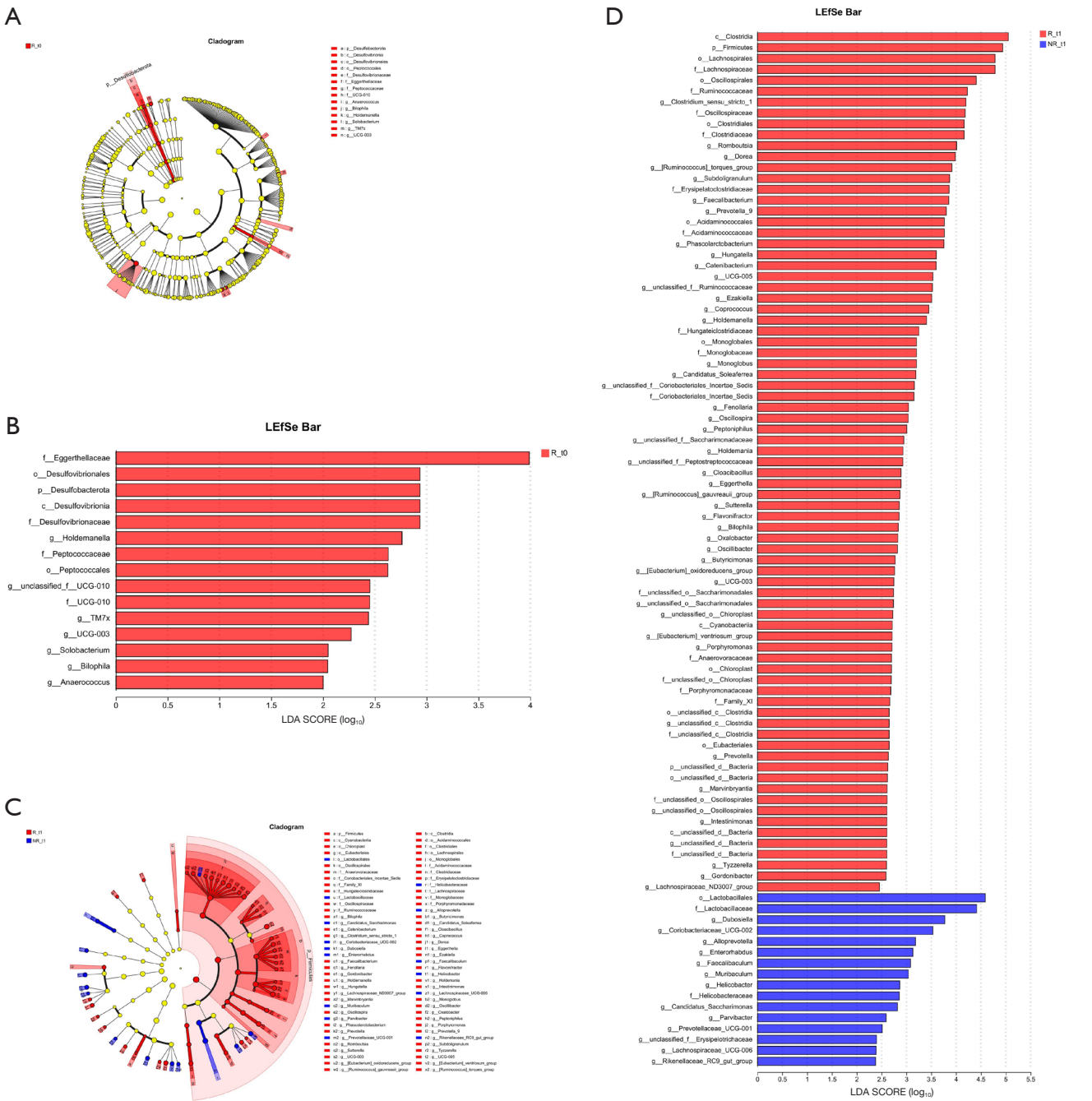

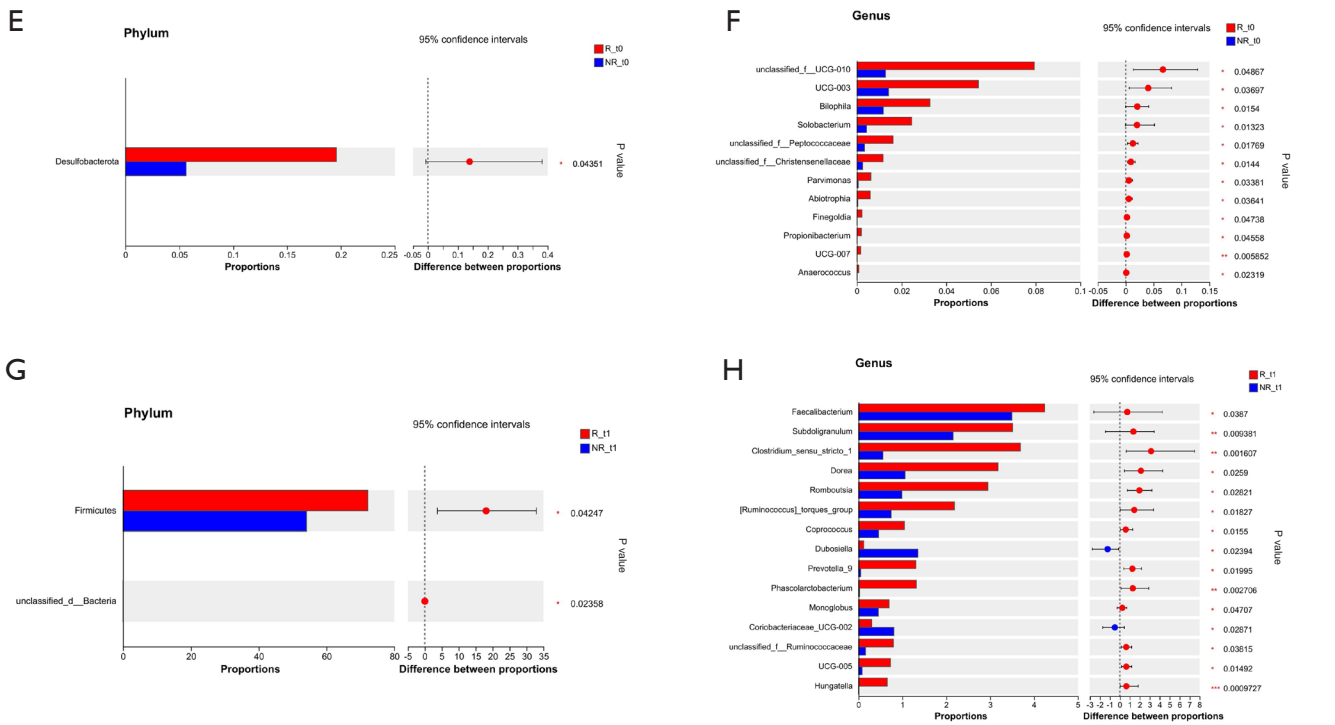

Figure 4 Gut microbiome composition associated with treatment response. (A) Taxonomic cladogram stratified in the R and NR groups at the baseline. (B) Differential abundance analysis using LEfSe stratified at the baseline. All the reported LEfSe findings are statistically significant. (C) Taxonomic cladogram stratified at the t1 timepoint. (D) Differential abundance analysis using LEfSe stratified at the t1 timepoint. All the reported LEfSe findings are statistically significant. (E) Differential microbiome at the phylum level between the R and NR groups at the baseline. (F) Differential microbiome at the genus level between the R and NR groups at the baseline. (G) Differential microbiome at the phylum level between the R and NR groups at the t1 timepoint. (H) Differential microbiome at the genus level between the R and NR groups at the t1 timepoint. Differential microbial score chart: the higher the score, the greater the contribution of the microbe to the difference. *, P<0.05; **, P<0.01; ***, P<0.001. R, responder; NR, non-responder; t0, baseline; t1, post-treatment; LEfSe, linear discriminant analysis effect sizes; LDA, linear discriminant analysis.

Database (HMDB; https://hmdb.ca/) revealed that a majority of the metabolites were up-regulated at the t0 timepoint, including 45 kinds of lipids and lipid-like molecules (33.58%), such as cholylmethionine, chenodeoxycholylphenylalanine, and ursodeoxycholic acid 3-sulfate, and 23 kinds of organic acids and derivatives (17.16%), such as glucose-6-glutamate, asparaginyl-phenylalanine, and proctolin. The down-regulated metabolites mainly comprised 23 kinds of organoheterocyclic compounds (22.77%), including 7'-carboxy-gamma-tocotrienol, penitrem E, and erinapyrone C, and 22 kinds of lipids and lipid-like molecules (21.78%), including 5-acetamidovalerate, pentadecanoic acid, and deoxycholic acid 3-glucuronide (*Figure 6A*). Conversely, the up-regulated compounds accounted for a minority of the metabolites at the t1 timepoint, and mainly included 23 kinds of lipids and lipid-like molecules, such as 2-methoxyestrone 3-glucuronide, ganosporeric acid A, and ichangic acid 17-beta-d-glucopyranoside, and 22 kinds of organic acids and derivatives (22.92%), such as 5-amino-6-ribitylamino uracil, dihydromelilotoside, and 4-hydroxy ketorolac. The down-regulated metabolites mainly included 33 kinds of organic acids and derivatives (30.00%), such as 4-(4-hydroxyphenyl)-2-butanone glucoside, alpha-L-arabinofuranose, and cyclopentanol, and 30 kinds of organoheterocyclic compounds (27.27%), such as 5,7-dihydroxy-4H-1-benzopyran-4-one, alpha-(chloromethyl)-2-hydroxymethyl-5-nitroimidazole-1-ethanol, and 5-phenylhydantoin (*Figure 6B*). On the whole, we also found a significant enrichment of SCFAs in the R group differential metabolites after immunotherapy (*Figure 6C-6E*).

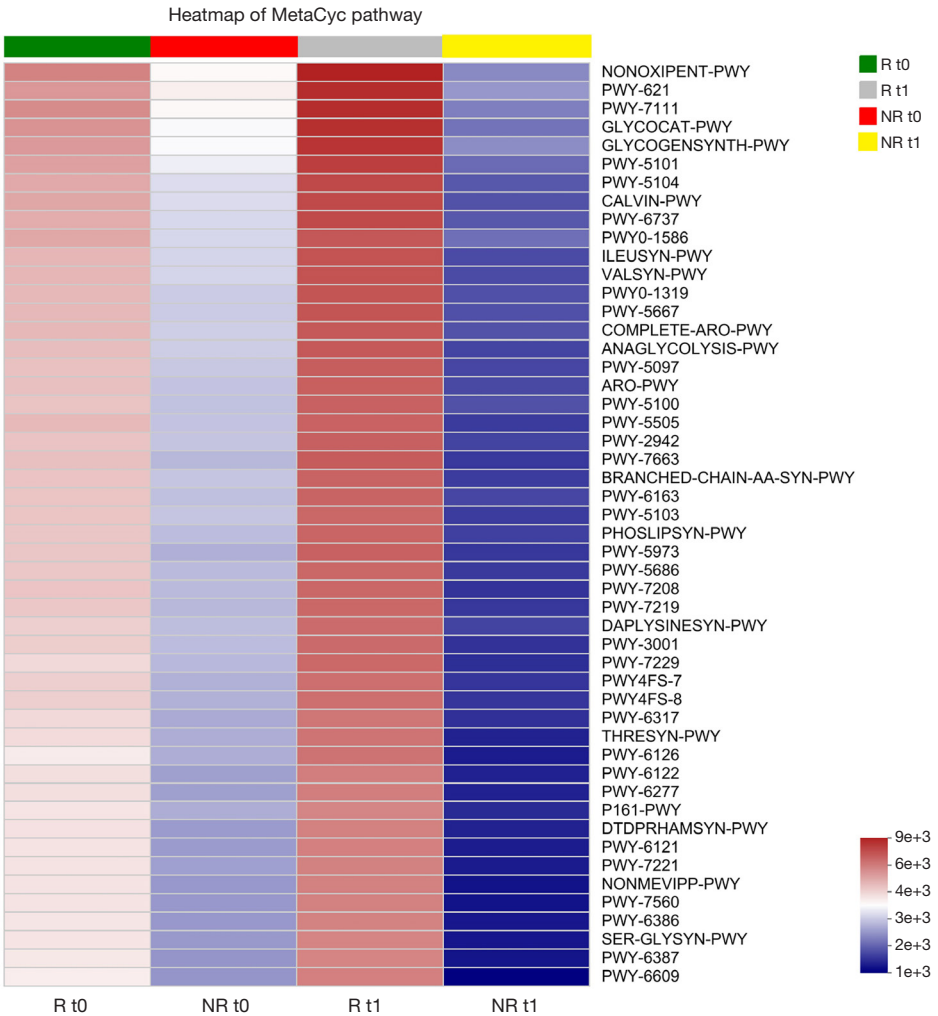

Figure 5 Heatmap of the differential bacteria functional pathways between the R and NR groups at the baseline and t1 timepoint. The color of each rectangle represents the coefficient value calculated by the MetaCyc analysis: red indicates high taxon richness; blue indicates low taxon richness. R, responder; NR, non-responder; t0, baseline; t1, post-treatment.

To gain a better understanding of the role played by the differential metabolites, we conducted a KEGG pathway enrichment analysis (*Figure 6F,6G*). The results showed that the differential metabolites in the R and NR groups at the baseline were mainly involved in glycerophospholipid metabolism, tyrosine metabolism, and the vascular endothelial growth factor (VEGF) signaling pathway (*Figure 6F*). After immunotherapy, the differential metabolites in the two groups were mainly involved in 20 pathways, including sphingomyelin metabolism, arginine biosynthesis, the nuclear factor (NF)-kappa B signaling pathway, type 1 T helper (Th1) and type 2 T helper (Th2) cell differentiation, lysine biosynthesis, the PD-L1 expression and PD-1 checkpoint pathway in cancer, type 17 T helper (Th17) cell differentiation, natural killer cell-mediated cytotoxicity, the B cell receptor signaling pathway, and the T cell receptor signaling pathway.

Multi-omics analysis revealed a correlation between ICI response and the gut microbiota and its metabolites

Further, we investigated the interactions between differential flora and differential metabolites separately in the two groups. The results showed that at the baseline level, the abundance of *g_Propionibacterium*, *g_Solobacterium*, and *g_Parvimonas* was negatively correlated with some

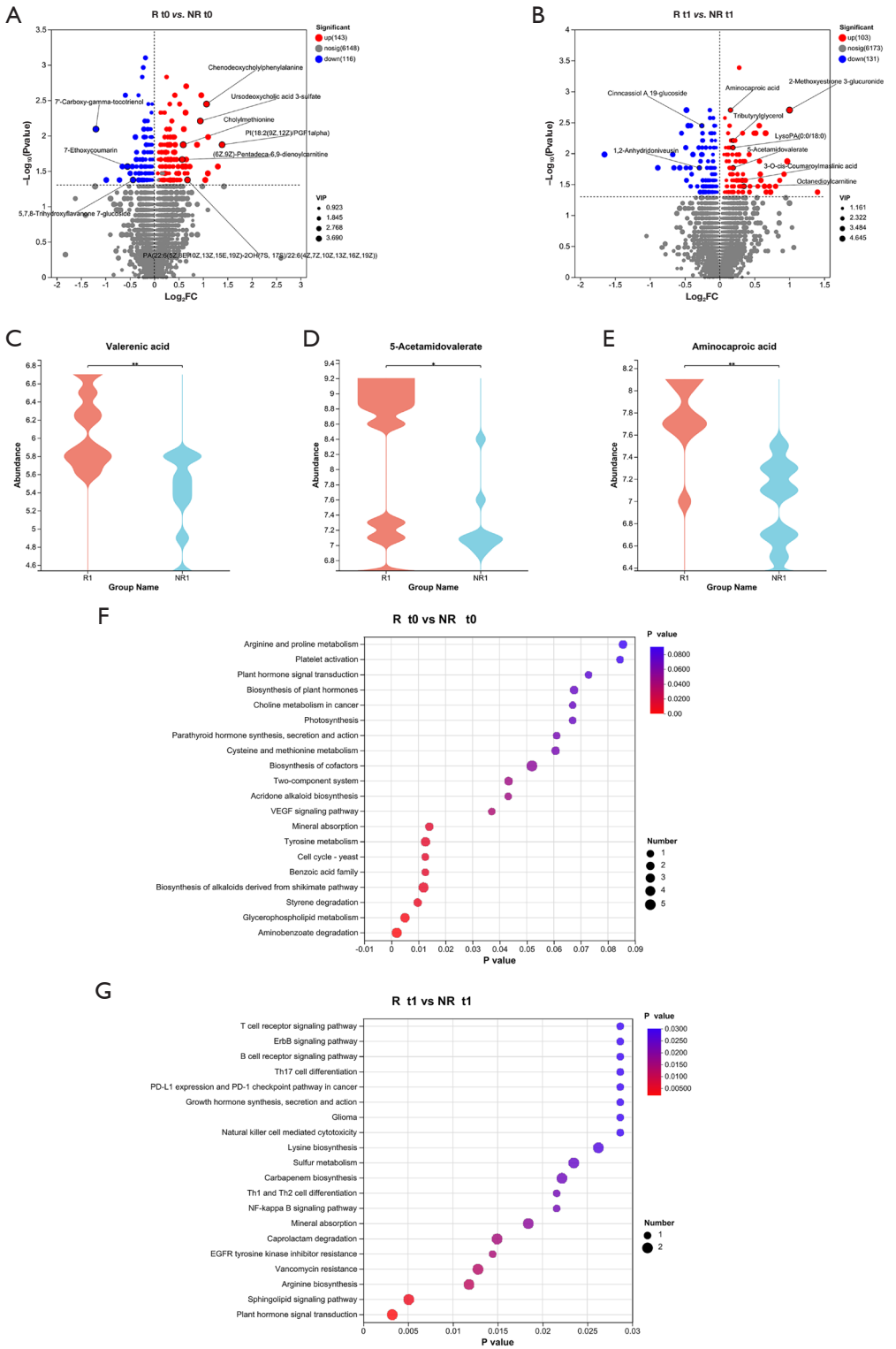

Figure 6 General overview of the metabolome. (A) Volcano plot showing the significant different metabolites between the R and NR groups at the baseline. The blue dots on the left are down-regulated metabolites; the red dots on the right are the up-regulated metabolites; the grey dots are the metabolites that are not significantly different. (B) Volcano plot showing the significant different metabolites between

the R and NR groups at the t1 timepoint. The blue dots on the left are down-regulated metabolites; the red dots on the right are the up-regulated metabolites; the grey dots are the metabolites that are not significantly different. (C-E) The Wilcoxon test results showed that the abundance of three SCFAs in the R and NR groups changed at the t1 time point. *, P<0.05; **, P<0.01. (F) The KEGG pathway enrichment analysis of the LC-MS metabolites in the feces samples of the R and NR groups at the baseline. (G) The KEGG pathway enrichment analysis of the LC-MS metabolites in the feces samples of the R and NR groups at the t1 timepoint. R, responder; NR, non-responder; t0, baseline; t1, post-treatment; FC, fold change; VIP, variable importance in the projection; SCFA, short-chain fatty acid; KEGG, Kyoto Encyclopedia of Genes and Genomes; LC-MS, liquid chromatography-mass spectrometry.

lipid analogs, such as dodecanol, palmitic amid, and 1-hexadecanol geranic acid, and the remaining genera were positively correlated with metabolites. At the t1 timepoint, the differential genera enriched in the R group were mostly associated with the top 50 differential metabolites in abundance, such as tributyrylglycerol, aminocaproic acid, sayanedin, and 2-methoxyestrone 3-glucuronide (*Figure 7A*), while *g_Dubosiella* and *g_Coriobacteriaceae_UCG-002* were positively correlated with the metabolites. Given that the metabolites involved in the differential metabolic pathway were found to be mainly lipid and amino acid-based, we examined the correlation between the differential microbiota and lipid and amino acid-based differential metabolites, and found that the differential microbiota that were enriched in the R group, such as *g_Hungatella* and *g_Faecalibacterium*, were mainly positively correlated with lipid-based metabolites, and were negatively correlated with amino acid-based metabolites (*Figure 7B*).

Discussion

ES-SCLC is considered a refractory carcinoma with extremely rapid disease progression. After more than three decades without clinical advances, research on ICIs combined with platinum-based chemotherapy has led to the first treatment breakthrough and the establishment of a new standard for the first-line treatment for ES-SCLC. However, not all patients can benefit from ICIs; thus, there is an urgent need to discover important regulators of ICI-induced anti-tumor immune responses (20). The microbiome has been found to play a significant role in ICIs for various tumors, but the relevant research has been less in SCLC tumor species (18). In this study, we conducted a comprehensive analysis of gut microbiota and metabolite profiles in Chinese ES-SCLC patients receiving ICI treatment.

Gut microbiome diversity is defined as the distribution of the number and abundance of different types of microorganisms that colonize the gut (21,22). Abnormal diversity of the gut microbiome has been shown to profoundly influence the immune system, thereby affecting the efficacy of ICIs (23,24). Our study revealed that the R and NR patients had similar levels of alpha and beta diversity at the baseline. However, after receiving ICI treatment, we observed that alpha and beta diversity were significantly higher in the R group than the NR group. This implies that immunotherapy benefits were linked to an increased gut microbiome diversity. Recently, Gopalakrishnan *et al.* examined the relationship between the gut microbiome and clinical responses to ICIs in melanoma patients, and found that higher alpha diversity was associated with immunotherapy response (25). Jin *et al.* also examined the relationship between the diversity of the gut microbiome and clinical outcomes in Chinese NSCLC patients receiving anti-PD-1 immunotherapy, and found that patients who responded well to treatment had a higher diversity of gut microbiome at the starting point and a stable composition during treatment (26). These findings are broadly consistent with our findings. The above findings all suggest that gut microbiota diversity could be a co-beneficial factor for ICI treatment, regardless of the genetic background, geographical location, lifestyle, and diet of the patient.

Although there was no statistically significant difference in bacterial diversity between the two groups at baseline, it could not be ruled out that the existence of relevant different bacterial genera affected the antitumor treatment efficacy between the two groups. A study has shown that the use of live bacterial product *Clostridium butyricum* MIYAIRI 588 is related to the survival rate of advanced LC patients receiving chemotherapy combined with immunotherapy (27). Therefore, we have studied the gut microbiota composition and different microflora of the two groups of patients. And the results suggest that gut microbiome composition is associated with a favorable response to ICI treatment. At the baseline, *Firmicutes* and *Bacteroidetes* were less abundant in the R group, while *Proteobacteria* was more abundant. After immunotherapy, the abundance of *Firmicutes* and *Bacteroidetes* increased

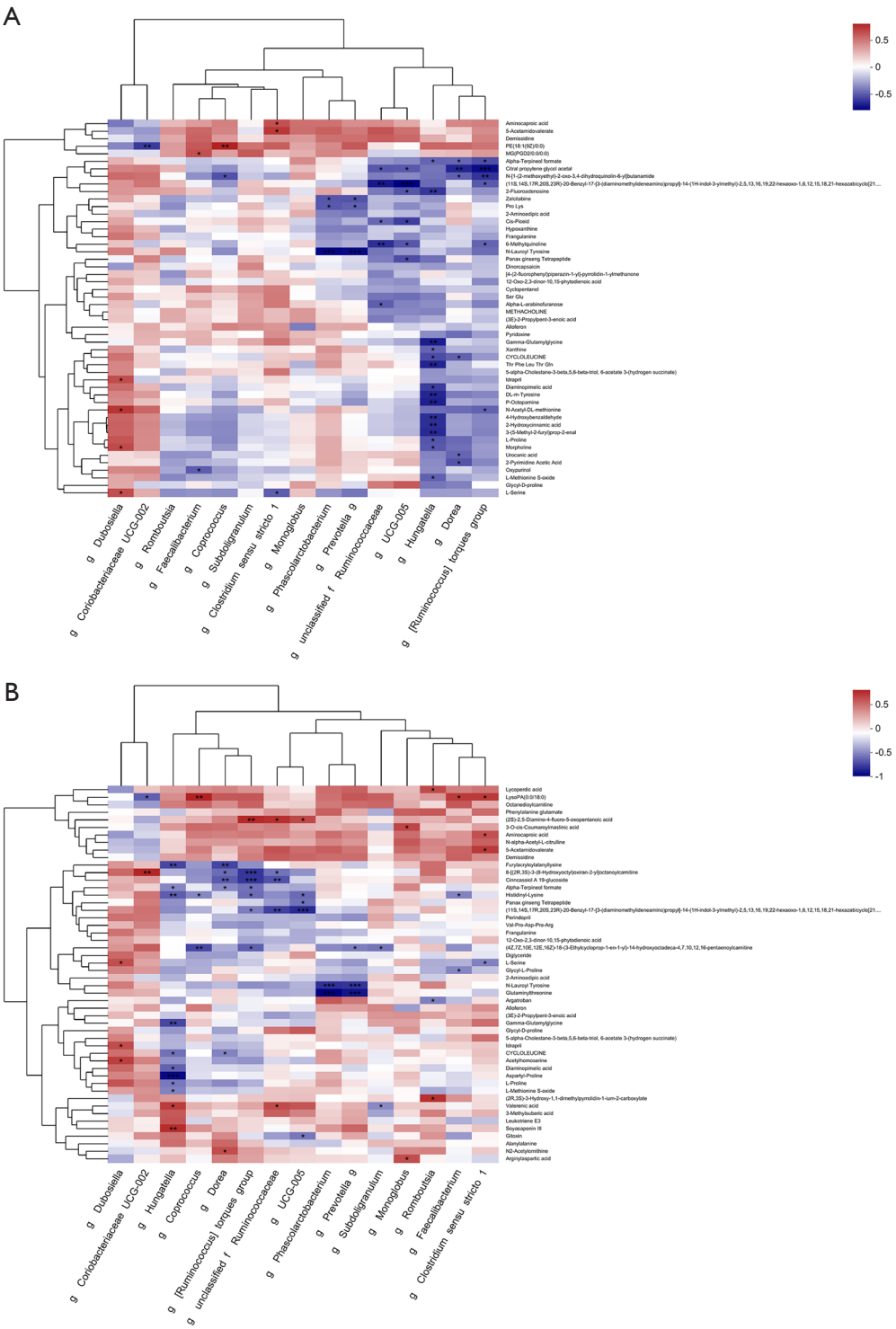

Figure 7 Multi-omics approaches revealed microbiota-metabolite interactions in ES-SCLC patients. Heatmap showing the correlation between 15 differential genera and differential metabolites (based on a Spearman's correlation analysis). *, P<0.05; **, P<0.01; ***, P<0.001. (A) Correlation analysis between 15 differential genera and the top 50 differential metabolites in abundance. (B) Correlation analysis between 15 different genera and different metabolites of lipids and amino acids. ES-SCLC, extensive-stage small cell lung cancer.

in the R group, while the abundance of *Proteobacteria* decreased. However, there was no significant change in the intestinal flora composition in the NR group before and after immunotherapy. A previous study has confirmed that *Firmicutes* and *Bacteroidetes* decompose carbohydrates in the colon and produce SCFAs, among which *Firmicutes* mainly produce butyrate, and *Bacteroidetes* mainly produce acetate and propionate (28). Butyrate inhibits the proliferation of LC cells by regulating p21 expression, while propionate inhibits cell growth by inducing apoptosis and cell cycle arrest (29). Moreover, Liu *et al.* reported that *Proteobacteria* is a potential pathogen of intestinal dysbiosis in LC patients (9), producing genotoxins and virulence factors that promote inflammation and carcinogenesis by activating Toll- or Nod-like receptors (30,31). This suggests that there may be a potential relationship between gut microbiota composition and the effectiveness of ICIs in treating SCLC patients. As changes in the F/B ratio are often considered to be relevant to ecological dysbiosis, they are also often used to assess the characteristics of the intestinal flora in patients with cancer (32). Several studies suggested that a decrease in the F/B ratio may be linked to the progression and recurrence of breast cancer (33) and colorectal cancer (34). In our study, the F/B ratio in both the R and NR groups displayed a downward trend after immunotherapy, which may be related to the characteristics of high malignancy and easy recurrence of SCLC. At the same time, *Blautia* was found to be significantly higher in the R group than in the NR group after treatment, therefore, we speculated that *Blautia* was related to immunotherapy benefits in SCLC patients. A recent study has shown that *Blautia*, which is an important bacterium in our intestines, produces acetate that provides energy for intestinal epithelial cells and has anti-inflammatory properties (35). Additionally, *Blautia* has been found to be less abundant in the intestinal flora of patients with colorectal cancer, which further supports our conclusion (36).

To further explore the correlation between specific differential gut microbiota and responses to ICIs, we applied LefSe and LDA scores and the Wilcoxon rank-sum test, respectively, to analyze the characteristic and differential microbiota between the R and NR groups at the t0 and t1 timepoints, and the results showed some overlap. At the baseline, *Desulfobacterota* at the phylum level was significantly enriched in the R group. As a sulfate-reducing bacterium, *Desulfobacterota* is widely believed to be harmful to humans; however, a study has found that *Desulfobacterota* is significantly more abundant in the feces of normal individuals than that of NSCLC patients (37). Furthermore, research indicates that *Desulfobacterota* can produce acetic acid by consuming lactic acid, and can become symbiotic with *Faecalibacterium prausnitzii*, which produces lactic acid, resulting in more SCFAs, and SCFAs help mobilize the body's immune response (38).

Before ICI treatment, we also detected 12 different bacteria at the genus level, all of which were enriched in the R group. Interestingly, in our study, most of the bacteria enriched in the R group were pro-inflammatory gram-negative bacteria. A previous study has reported an association between gram-negative bacteria, such as *Akkermansia muciniphila*, *Alistipes*, and *Porphyromonas*, and a better clinical response to immunotherapy (39). After ICI treatment, *Firmicutes* was enriched at the phylum level, and the following 13 species of bacteria were enriched at the genus level in the R group: *Faecalibacterium*, *Subdoligranulum*, *Clostridium_sensu_stricto_1*, *Dorea*, *Romboutsia*, *(Ruminococcus)_torques_*, *Coprococcus*, *Prevotella_9*, *Phascolarctobacterium*, *Monoglobus*, *unclassified_f_Ruminococcaceae*, *UCG-005*, and *Hungatella*. While the following two species of bacteria were enriched in the NR group: *Dubosiella* and *Coriobacteriaceae_UCG-002*. *Faecalibacterium*, *Subdoligranulum*, *Phascolarctobacterium*, *Coprococcus*, and *Ruminococcus* are highly active transcriptionally, and potentially metabolically. These bacteria are all producers of butyrate, which is critical to the host in terms of metabolism and immunity, especially in the case of some metabolic disorders and some autoimmune diseases (40-42). Conversely, *Coriobacteriaceae UCG-002*, which was enriched in the NR group, belongs to the Rhodiaceae family and can produce phenol and p-cresol, both of which are cytotoxic and reduce intestinal barrier function (43). Therefore, we speculate that the increase of intestinal SCFA flora in SCLC patients is associated with ICI treatment benefits, and may be a potential marker for predicting the efficacy of ICIs.

It is not yet known how the diversity of gut microbiota affects the systemic immune response. Thus, we used the PICRUST2 software to predict the microbial function of patients in the R group. The results of the gut microbiota functional pathway predicted at the MetaCyc pathway level showed that the microbiota function of the ICI respondents was mainly focused on amino acid and lipid metabolism. This is consistent with previous findings that microbiome-derived SCFAs and other metabolites are good candidates for powerful immunomodulatory effects (44). In the future, we will focus our research on analyzing the relevant metabolites.

One way the gut microbiome affects the host is through metabolites. Primary metabolites, like nucleotides and amino acids, are involved in the cell's normal functions and energy metabolism. Secondary metabolites, which are formed from primary metabolites through enzymatic modifications, play an important role in gut-microbiome interactions. Amino acid-derived secondary metabolites, including those from aromatic amino acids and glutamate, are particularly diverse and significant (45). When performing the metabolomics analysis, we found that at both the baseline and post-treatment, the differential metabolites were mostly amino acids, lipids, and lipid-like molecules (e.g., cholylmethionine and 2-methoxyestrone 3-glucuronide) in the R group and ganosporeric acid A in the NR group.

As metabolites produced by *Firmicutes* and *Bacteroidetes*, SCFAs have been shown to improve intestinal barrier function and anti-inflammatory effects, and have also been widely shown to exert beneficial effects in tumor immunotherapy (46). It has been shown that SCFAs can facilitate the response to ICIs by increasing T cell activation while decreasing T cell depletion (46,47). Clinical data on immunotherapy for solid tumors, including NSCLC, has shown that high concentrations of SCFAs in feces and serum are associated with longer progression-free survival (48). However, we compared the SCFAs in the R and NR groups of in SCLC patients, and found that after immunotherapy, SCFAs, including valerenic acid, 5-acetamidovalerate, aminocaproic acid, and other metabolites were significantly up-regulated and positively correlated with *Clostridia*. In addition to SCFAs, medium- and long-chain fatty acids were also found to be enriched in the R group, and were also found to have a potential role in enhancing immunotherapy efficacy (49).

To understand the major biological roles of the differential metabolites in the organism, we performed a KEGG pathway enrichment analysis of the differential metabolites and found that of 39 differential pathways, the top 20 differential pathways included the sphingolipid signaling pathway, arginine biosynthesis, the NF-kappa B signaling pathway, Th1 and Th2 cell differentiation, lysine biosynthesis, the PD-L1 expression and PD-1 checkpoint pathway in cancer, Th17 cell differentiation, natural killer cell-mediated cytotoxicity, the B cell receptor signaling pathway, and the T cell receptor signaling pathway. These included the pathways necessary for the anti-tumor therapy of ICIs, including the lipid and amino acid pathways, and the pathways for the immune recognition of the killing process by T cells, B cells, and others.

It is well known that PD-L1 inhibitors work by blocking the binding of PD-L1 to PD-1 and CD80 (50), which enables tumor-infiltrating T cells to recognize and kill tumor cells; however, data have shown that less than 20% of SCLC patients have positive PD-L1 expression (51). In a cohort study of 102 patients with limited-stage SCLC (LS-SCLC) and ES-SCLC, researchers observed that PD-L1 expression independently predicted favorable outcomes in the ES-SCLC cohort (52). This evidence suggests that the PD-L1 expression and PD-1 checkpoint pathway in cancer is the core pathway of ICIs in the treatment of SCLC. Therefore, it has been speculated that *Faecalibacterium*, *Hungatella*, and other bacteria regulate the PD-L1 expression and PD-1 checkpoint pathway in cancer, the Th1, Th2, and Th17 cell differentiation pathway, and the T and b cell signaling pathway in tumors by producing metabolites such as SCFAs. Thus, ICIs could enhance anti-tumor activity by regulating a variety of immune cell populations and thus improve the efficacy of anti-tumor drugs.

Conclusions

Our study demonstrated that the gut microbiota and metabolites are associated with a favorable response to ICI therapy in ES-SCLC within Chinese cohorts. These findings suggest that modulating the gut microbiota prior to treatment could be a novel strategy to enhance the efficacy of ICI immunotherapy. However, further validation in a large cohort study is required. Our study is the first to provide evidence that the gut microbiota significantly influences ICI-induced anti-tumor immune responses in ES-SCLC.

Acknowledgments

We are indebted to all the patients who participated in this study, and to the graduate students and teachers at the Department of Oncology of the Affiliated Hospital of Qingdao University, China.

Funding: This work was supported by the Qingdao Natural Science Foundation (No. 23-2-1-189-zyyd-jch to J.W.), the Wu Jieping Medical Foundation (No. 320.6750.2021-02-92 to Z.Y.), and the Shandong Provincial Medical Association (No. YXH2022ZX02020 to Z.Y.).

Footnote

Reporting Checklist: The authors have completed the MDAR

reporting checklist. Available at https://jtd.amegroups.com/article/view/10.21037/jtd-24-1201/rc

Data Sharing Statement: Available at https://jtd.amegroups.com/article/view/10.21037/jtd-24-1201/dss

Peer Review File: Available at https://jtd.amegroups.com/article/view/10.21037/jtd-24-1201/prf

Conflicts of Interest: All authors have completed the ICMJE uniform disclosure form (available at https://jtd.amegroups.com/article/view/10.21037/jtd-24-1201/coif). The authors have no conflicts of interest to declare.

Ethical Statement: The authors are accountable for all aspects of the work in ensuring that questions related to the accuracy or integrity of any part of the work are appropriately investigated and resolved. The Ethics Committee of the Affiliated Hospital of Qingdao University approved the study of fecal samples from ES-SCLC patients (ethics number: QYFY WZLL 27469). This study was conducted in accordance with the Declaration of Helsinki (as revised in 2013). All the patients were informed of the study and provided informed consent.

References

1. Siegel RL, Miller KD, Wagle NS, et al. Cancer statistics, 2023. CA Cancer J Clin 2023;73:17-48.
2. Meijer JJ, Leonetti A, Airò G, et al. Small cell lung cancer: Novel treatments beyond immunotherapy. Semin Cancer Biol 2022;86:376-85.
3. Lee JH, Saxena A, Giaccone G. Advancements in small cell lung cancer. Semin Cancer Biol 2023;93:123-8.
4. Zugazagoitia J, Paz-Ares L. Extensive-Stage Small-Cell Lung Cancer: First-Line and Second-Line Treatment Options. J Clin Oncol 2022;40:671-80.
5. Yang S, Zhang Z, Wang Q. Emerging therapies for small cell lung cancer. J Hematol Oncol 2019;12:47.
6. Ganti AKP, Loo BW, Bassetti M, et al. Small Cell Lung Cancer, Version 2.2022, NCCN Clinical Practice Guidelines in Oncology. J Natl Compr Canc Netw 2021;19:1441-64.
7. Mamdani H, Matosevic S, Khalid AB, et al. Immunotherapy in Lung Cancer: Current Landscape and Future Directions. Front Immunol 2022;13:823618.
8. Ni Y, Lohinai Z, Heshiki Y, et al. Distinct composition and metabolic functions of human gut microbiota are associated with cachexia in lung cancer patients. ISME J 2021;15:3207-20.
9. Liu F, Li J, Guan Y, et al. Dysbiosis of the Gut Microbiome is associated with Tumor Biomarkers in Lung Cancer. Int J Biol Sci 2019;15:2381-92.
10. Ge Y, Wang X, Guo Y, et al. Gut microbiota influence tumor development and Alter interactions with the human immune system. J Exp Clin Cancer Res 2021;40:42.
11. Roviello G, Iannone LF, Bersanelli M, et al. The gut microbiome and efficacy of cancer immunotherapy. Pharmacol Ther 2022;231:107973.
12. Routy B, Le Chatelier E, Derosa L, et al. Gut microbiome influences efficacy of PD-1-based immunotherapy against epithelial tumors. Science 2018;359:91-7.
13. Lee KA, Thomas AM, Bolte LA, et al. Cross-cohort gut microbiome associations with immune checkpoint inhibitor response in advanced melanoma. Nat Med 2022;28:535-44.
14. Hakozaki T, Richard C, Elkrief A, et al. The Gut Microbiome Associates with Immune Checkpoint Inhibition Outcomes in Patients with Advanced Non-Small Cell Lung Cancer. Cancer Immunol Res 2020;8:1243-50.
15. Derosa L, Hellmann MD, Spaziano M, et al. Negative association of antibiotics on clinical activity of immune checkpoint inhibitors in patients with advanced renal cell and non-small-cell lung cancer. Ann Oncol 2018;29:1437-44.
16. Bender MJ, McPherson AC, Phelps CM, et al. Dietary tryptophan metabolite released by intratumoral Lactobacillus reuteri facilitates immune checkpoint inhibitor treatment. Cell 2023;186:1846-1862.e26.
17. Botticelli A, Vernocchi P, Marini F, et al. Gut metabolomics profiling of non-small cell lung cancer (NSCLC) patients under immunotherapy treatment. J Transl Med 2020;18:49.
18. Lu Y, Yuan X, Wang M, et al. Gut microbiota influence immunotherapy responses: mechanisms and therapeutic

strategies. J Hematol Oncol 2022;15:47.
19. Chen S, Gui R, Zhou XH, et al. Combined Microbiome and Metabolome Analysis Reveals a Novel Interplay Between Intestinal Flora and Serum Metabolites in Lung Cancer. Front Cell Infect Microbiol 2022;12:885093.
20. Iams WT, Porter J, Horn L. Immunotherapeutic approaches for small-cell lung cancer. Nat Rev Clin Oncol 2020;17:300-12.
21. Li X, Zhang S, Guo G, et al. Gut microbiome in modulating immune checkpoint inhibitors. EBioMedicine 2022;82:104163.
22. Yi M, Yu S, Qin S, et al. Gut microbiome modulates efficacy of immune checkpoint inhibitors. J Hematol Oncol 2018;11:47.
23. Oh B, Boyle F, Pavlakis N, et al. The Gut Microbiome and Cancer Immunotherapy: Can We Use the Gut Microbiome as a Predictive Biomarker for Clinical Response in Cancer Immunotherapy? Cancers (Basel) 2021;13:4824.
24. Sun JY, Yin TL, Zhou J, et al. Gut microbiome and cancer immunotherapy. J Cell Physiol 2020;235:4082-8.
25. Gopalakrishnan V, Spencer CN, Nezi L, et al. Gut microbiome modulates response to anti-PD-1 immunotherapy in melanoma patients. Science 2018;359:97-103.
26. Jin Y, Dong H, Xia L, et al. The Diversity of Gut Microbiome is Associated With Favorable Responses to Anti-Programmed Death 1 Immunotherapy in Chinese Patients With NSCLC. J Thorac Oncol 2019;14:1378-89.
27. Tomita Y, Sakata S, Imamura K, et al. Association of Clostridium butyricum Therapy Using the Live Bacterial Product CBM588 with the Survival of Patients with Lung Cancer Receiving Chemoimmunotherapy Combinations. Cancers (Basel) 2023;16:47.
28. Allers K, Stahl-Hennig C, Fiedler T, et al. The colonic mucosa-associated microbiome in SIV infection: shift towards Bacteroidetes coincides with mucosal CD4(+) T cell depletion and enterocyte damage. Sci Rep 2020;10:10887.
29. Mowday AM, Dubois LJ, Kubiak AM, et al. Use of an optimised enzyme/prodrug combination for Clostridia directed enzyme prodrug therapy induces a significant growth delay in necrotic tumours. Cancer Gene Ther 2022;29:178-88.
30. Schwabe RF, Jobin C. The microbiome and cancer. Nat Rev Cancer 2013;13:800-12.
31. Bingula R, Filaire E, Molnar I, et al. Characterisation of microbiota in saliva, bronchoalveolar lavage fluid, non-malignant, peritumoural and tumour tissue in non-small cell lung cancer patients: a cross-sectional clinical trial. Respir Res 2020;21:129.
32. Xi Y, Liu F, Qiu B, et al. Analysis of Gut Microbiota Signature and Microbe-Disease Progression Associations in Locally Advanced Non-Small Cell Lung Cancer Patients Treated With Concurrent Chemoradiotherapy. Front Cell Infect Microbiol 2022;12:892401.
33. Okubo R, Kinoshita T, Katsumata N, et al. Impact of chemotherapy on the association between fear of cancer recurrence and the gut microbiota in breast cancer survivors. Brain Behav Immun 2020;85:186-91.
34. Gao R, Kong C, Huang L, et al. Mucosa-associated microbiota signature in colorectal cancer. Eur J Clin Microbiol Infect Dis 2017;36:2073-83.
35. Qingbo L, Jing Z, Zhanbo Q, et al. Identification of enterotype and its predictive value for patients with colorectal cancer. Gut Pathog 2024;16:12.
36. Zhang X, Yu D, Wu D, et al. Tissue-resident Lachnospiraceae family bacteria protect against colorectal carcinogenesis by promoting tumor immune surveillance. Cell Host Microbe 2023;31:418-432.e8.
37. Ni B, Kong X, Yan Y, et al. Combined analysis of gut microbiome and serum metabolomics reveals novel biomarkers in patients with early-stage non-small cell lung cancer. Front Cell Infect Microbiol 2023;13:1091825.
38. Chen YR, Jing QL, Chen FL, et al. Desulfovibrio is not always associated with adverse health effects in the Guangdong Gut Microbiome Project. PeerJ 2021;9:e12033.
39. Derosa L, Routy B, Thomas AM, et al. Intestinal Akkermansia muciniphila predicts clinical response to PD-1 blockade in patients with advanced non-small-cell lung cancer. Nat Med 2022;28:315-24.
40. Liu X, Dai M, Ma Y, et al. Reconstruction and Dynamics of the Human Intestinal Microbiome Observed In Situ. Engineering. 2022;15:89-101.
41. Wu F, Guo X, Zhang J, et al. Phascolarctobacterium faecium abundant colonization in human gastrointestinal tract. Exp Ther Med 2017;14:3122-6.
42. Rivière A, Selak M, Lantin D, et al. Bifidobacteria and Butyrate-Producing Colon Bacteria: Importance and Strategies for Their Stimulation in the Human Gut. Front Microbiol 2016;7:979.
43. Yu Z, Li D, Sun H. Herba Origani alleviated DSS-induced ulcerative colitis in mice through remolding gut microbiota to regulate bile acid and short-chain fatty acid metabolisms. Biomed Pharmacother 2023;161:114409.

44. Hersi F, Elgendy SM, Al Shamma SA, et al. Cancer immunotherapy resistance: The impact of microbiome-derived short-chain fatty acids and other emerging metabolites. Life Sci 2022;300:120573.
45. Kuziel GA, Rakoff-Nahoum S. The gut microbiome. Curr Biol 2022;32:R257-64.
46. Blake SJ, Wolf Y, Boursi B, et al. Role of the microbiota in response to and recovery from cancer therapy. Nat Rev Immunol 2024;24:308-25.
47. He Y, Fu L, Li Y, et al. Gut microbial metabolites facilitate anticancer therapy efficacy by modulating cytotoxic CD8(+) T cell immunity. Cell Metab 2021;33:988-1000.e7.
48. Nomura M, Nagatomo R, Doi K, et al. Association of Short-Chain Fatty Acids in the Gut Microbiome With Clinical Response to Treatment With Nivolumab or Pembrolizumab in Patients With Solid Cancer Tumors. JAMA Netw Open 2020;3:e202895.
49. Westheim AJF, Stoffels LM, Dubois LJ, et al. Fatty Acids as a Tool to Boost Cancer Immunotherapy Efficacy. Front Nutr 2022;9:868436.
50. Zhang Y, Song Q, Cassady K, et al. Blockade of trans PD-L1 interaction with CD80 augments antitumor immunity. Proc Natl Acad Sci U S A 2023;120:e2205085120.
51. Antonia SJ, López-Martin JA, Bendell J, et al. Nivolumab alone and nivolumab plus ipilimumab in recurrent small-cell lung cancer (CheckMate 032): a multicentre, open-label, phase 1/2 trial. Lancet Oncol 2016;17:883-95.
52. Ishii H, Azuma K, Kawahara A, et al. Significance of programmed cell death-ligand 1 expression and its association with survival in patients with small cell lung cancer. J Thorac Oncol 2015;10:426-30.

(English Language Editor: L. Huleatt)

Cite this article as: Sun L, Wang X, Zhou H, Li R, Meng M, Roviello G, Oh B, Feng L, Yu Z, Wang J. Gut microbiota and metabolites associated with immunotherapy efficacy in extensive-stage small cell lung cancer: a pilot study. J Thorac Dis 2024;16(10):6936-6954. doi: 10.21037/jtd-24-1201